Ceramics-Silikáty 69 (3), 374-380 (2025)
www.ceramics-silikaty.cz doi: 10.13168/cs.2025.0021

# SYNTHESIS AND CHARACTERISATION OF ZNO-BASED NANOFIBRE MEMBRANES DOPED WITH ALUMINIUM AND COBALT USING THE ELECTROSPINNING METHOD

ADE IRVAN TAUVANA*,**, #GUNAWARMAN GUNAWARMAN *, YULI YETRI***, BAMBANG WAHONO****, LUKMAN NULHAKIM**

*Mechanical Engineering Dept., Universitas Andalas, Kampus Limau Manis, Padang 25163, Indonesia
**Manufacturing Engineering Technology Dept., Politeknik Engineering Indorama, Purw 41152, Indonesia
***Mechanical Engineering Dept., Politeknik Negeri Padang, 25163, Indonesia
**** National Research and Innovation Agency (BRIN) Indonesia

#E-mail: gunawarman@eng.unand.ac.id

Submitted February 12, 2025 accepted March, 2025

**Keywords:** Nanofibre, Electrospinning, Piezoelectric, Morphology, Nanogenerator

*Electrospun ZnO-based nanofibre membranes doped with $AlCl_3$ and CoAc were successfully fabricated for piezoelectric nanogenerator applications. The PVA precursor solution was prepared by dissolving PVA in distilled water and then processed using an electrospinning machine for 10 hours. Characterisation of the nanofibres was performed using scanning electron microscopy (SEM), energy-dispersive X-ray spectroscopy (EDX), X-ray diffraction (XRD), and Fourier Transform Infrared Spectroscopy (FTIR) to examine the fibre and membrane properties. The SEM analysis revealed that the incorporation of Al and Co influenced the fibre morphology and size. The EDX confirmed the presence of Al and Co in the nanofibre membranes. The XRD results indicated that all the membranes exhibited an amorphous structure, while the FTIR analysis confirmed the complete evaporation of the solvent during the spinning process. The presence of a metal-oxygen phase plays a crucial role in analysing the crystal structure and piezoelectric characteristics of the material.*

## INTRODUCTION

The depletion of natural fossil energy reserves continues to accelerate due to the ongoing exploration to meet global energy demands. Renewable energy sources, including mechanical vibrations, noise, heat, wave motion, geothermal energy, wind, and solar power, still require further advancements [1]. Among these, mechanical energy can be converted into electrical energy using piezoelectric materials. However, the vast availability of mechanical energy in nature remains underutilised. In recent years, the development of piezoelectric nanogenerators (PENGs) has gained significant attention from researchers due to their potential as self-sustaining power sources for portable electronic devices, addressing the increasing demand for energy [1–3].

PENGs are made from piezoelectric materials with a non-centrosymmetric crystal structure, such as ZnO, PZT, and $BaTiO_3$ [4]. Zinc oxide (ZnO) is widely studied due to its excellent piezoelectric, pyroelectric, and optical properties [5]. Additionally, ZnO has a relatively wide band gap of 3.37 eV [6], is non-toxic [7], cost-effective, easily accessible [8], stable, and environmentally friendly [9]. However, ZnO-based PENGs typically suffer from low power output [10, 11] and limited stability [12]. One approach to enhancing the performance and stability of PENGs is utilising one-dimensional (1D) piezoelectric nanostructures, such as nanowires, nanorods, and nanofibres [9, 13, 14]. Among these, nanofibre-based PENGs offer several advantages, including excellent piezoelectric properties, high flexibility, and the ability to be integrated onto flexible substrates [3, 7]. Furthermore, nanofibres can absorb mechanical energy more effectively than spherical nanogenerators, as they allow for continuous mechanical force distribution from one fibre to another over an extended period [15].

Previous studies on ZnO-based nanowires as nanogenerators have demonstrated the ability to generate voltages of up to 25 mV [3]. Additionally, research on ZnO nanorods doped with aluminium (Al) has shown voltage outputs reaching 60 mV [4]. Further investigations have revealed that doping ZnO nanofibres with Al can enhance voltage generation up to 265.5 mV [5]. It has also been found that ZnO fibres can be modified with aluminium to form aluminium-doped zinc oxide (AZO) [6]. Moreover, nanofibre-based piezoelectric materials can be fabricated cost-effectively using the electrospinning method [7].

A higher precursor discharge during the electrospinning process can lead to larger fibre sizes, resulting in lower crystal material deformation. Consequently, lower deformation leads to reduced stress [8]. Additionally, previous research has shown that ZnO- and AZO-based nanogenerators (NGs) achieved maximum power densities of 12.9 and 38.8 $nW/cm^2$, respectively. However,

this power density remains low due to the brittle nature of zinc oxide [9], which prevents a voltage increase under high loads [10]. This study aims to enhance the performance of ZnO nanogenerators by incorporating additional dopants, specifically aluminium (Al) from $AlCl_3$ and cobalt (Co) from $Co_3O_4$.

Aluminium was selected because it can reduce ZnO fibres and has excellent electrical conductivity. Meanwhile, cobalt was chosen due to its modulus of elasticity, which is nearly three times higher than that of aluminium. This study focuses on doping ZnO with both aluminium and cobalt, aiming to enhance the performance of piezoelectric materials. Research on renewable energy, particularly in the development of advanced materials for energy harvesting, remains relatively limited compared to the broader scope of renewable energy studies. The primary objective of this research is to produce a piezoelectric material that serves as a key component in nanogenerators, enabling the conversion of mechanical energy into electrical energy.

## EXPERIMENTAL MATERIALS AND METHODS

### Material

The materials used in this study include zinc acetate dihydrate ($Zn(CH_3COO)_2 \cdot 2H_2O$, Merck), aluminium chloride hexahydrate ($AlCl_3 \cdot 6H_2O$, Merck), cobalt acetate tetrahydrate ($Co(CH_3COO)_2 \cdot 4H_2O$, Sigma Aldrich), polyvinyl alcohol (PVA, $(C_2H_4O)n$, molecular weight 72 000, Merck), and distilled water ($H_2O$), all of which were used without further purification. The fabrication of ZnO nanofibre (NFs)-based piezoelectric nanogenerators (PENGs) co-doped with cobalt and aluminium involves three main stages:

- Preparation of the precursor solution.
- Production of environmentally friendly nanofibres using the electrospinning technique.
- Characterisation of the synthesised PENG.

### Sample preparation

The PVA solution was prepared by dissolving PVA in $H_2O$ at a ratio of 1:10 (wt. %) and stirring at 70 °C for 4 hours, followed by an 8-hour rest period at room temperature. Meanwhile, the Zn:$AlCl_3$ and ZnAc:CoAc solutions with a 1:5 (wt. %) ratio were obtained by adding a mixture containing 10 % $AlCl_3$ and CoAc, with a total variation of 11 % by weight. Specifically, 4 g of each component was dissolved in 20 g of $H_2O$ and stirred at 70 °C for 1 hour. Subsequently, the ZnAc:$AlCl_3$ and ZnAc:CoAc solutions were each combined with PVA in a 1:4 (wt. %) ratio, stirred at 70 °C for 8 hours, and then left at room temperature for 24 hours. The ZnAc–$AlCl_3$ and ZnAc–CoAc solutions were then mixed in varying ZnAc–$AlCl_3$:ZnAc–CoAc ratios of 100:0, 75:25, 50:50, 25:75, and 0:100 (wt. %) of the total Al–Co composition. This process resulted in five transparent ZnAc–$AlCl_3$––CoAc:PVA solutions, which were subsequently used in the electrospinning process to produce nanofibres, as illustrated in Figure 1.

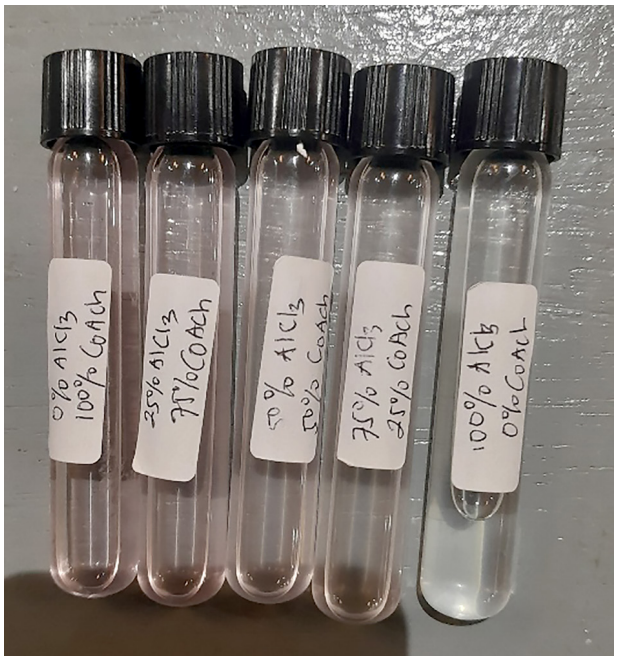


Figure 1. Solution sample.

### Electrospinning process

The prepared precursor solution was loaded into a 5 mL syringe, which was then mounted on a syringe pump to regulate the flow rate of the dispensed solution. The syringe was connected to a stainless-steel needle with a 0.65 mm diameter via silicone tubing. The rotary drum collector was grounded, while the stainless-steel needle was linked to a high-voltage (HV) power source. The generated nanofibres were collected on a nonwoven fibre membrane covering the rotary drum collector. The electrospinning process was conducted under specific parameters: an applied voltage of 13 kV, a 13 cm distance


Figure 2. Electrospinning machine.

between the drum collector and the needle tip, a solution flow rate of 0.5 mL/hour, a collector rotation speed of 125 rpm, and a controlled humidity of approximately 58 %. The electrospinning machine set-up is illustrated in Figure 2.

The nanofibre membrane, produced using an electrospinning machine with dimensions of 200 × 150 mm, is depicted in Figure 3.

### Characterisation of nanofibre membranes

The size and morphology of the nanofibre membrane were examined using a scanning electron microscope (SEM, JEOL, JSM IT300) at magnifications of 5000 and 50 000 times. The composition was analysed using an Energy-dispersive X-ray (EDX) detector. The X-ray diffraction (XRD) pattern of the nanofibre membrane was obtained with an X-ray diffractometer (Rigaku MiniFlex 600), with the diffraction recorded at 2θ angles ranging from 10° to 90°. The Fourier transform infrared (FTIR) spectra of the ZnAc:$AlCl_3$:PVA and ZnAc:CoAc:PVA nanofibre membranes were acquired using an FTIR spectrometer (Thermo Fisher Scientific NICOLET IS10FTIR). FTIR measurements were conducted within the wavenumber range of 500-4000 $cm^{-1}$.

## RESULTS AND DISCUSSION

### Scanning electron microscope (SEM) characterisation

The SEM analysis revealed the formation of nanofibres, with the results for samples (a) through (e) shown in Figure 4.

A SEM analysis was conducted at a magnification of 10 000× for the $AlCl_3$, CoAc, and Co-doped ZnO materials. The SEM images of ZnO doped with $AlCl_3$, shown in Figure 4, demonstrate that as the Al doping concentration increases, the resulting nanofibres become smaller. In contrast, ZnO doped with CoAc showed only a minor reduction in fibre size. Table 1 and Figure 4 display the fibre size distribution and SEM images of ZnO nanofibres co-doped with $AlCl_3$:CoAc, respectively.

a) b) c) d) e)

Figure 3. Electrospinning nanofibre membrane: a) 100 % $AlCl_3$, 0 % CoAc; b) 75 % $AlCl_3$, 25 % CoAc; c) 50 % $AlCl_3$, 50 % CoAc; d) 25 % $AlCl_3$, 75 % CoAc; e) 0 % $AlCl_3$, 1000 % CoAc.

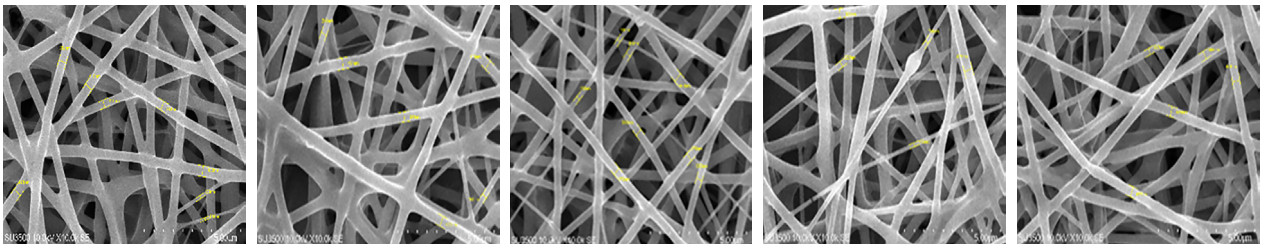

a) b) c) d) e)

Figure 4. SEM morphological analysis of: a) 100 % $AlCl_3$, 0 % CoAc; b) 75 % $AlCl_3$, 25 % CoAc; c) 50 % $AlCl_3$, 50 % CoAc; d) 25 % $AlCl_3$, 75 % CoAc; e) 0 % $AlCl_3$, 1000 % CoAc.

Table 1. Diameter of ZnO nanofibres with the Al–Co addition.

| Fibre diameter size | Fibre diameter size variations in Co-doping aluminium and cobalt | | | | |
|---|---|---|---|---|---|
| | 100 % $AlCl_3$ 0 % CoAc | 75 % $AlCl_3$ 25 % CoAc | 50 % $AlCl_3$ 50 % CoAc | 25 % $AlCl_3$ 75 % CoAc | 0 % $AlCl_3$ 100 % CoAc |
| Maximum (nm) | 424 | 442 | 451 | 411 | 458 |
| Minimum (nm) | 138 | 210 | 269 | 257 | 275 |
| Average (nm) | 341 | 344 | 363 | 365 | 361 |

In the case of co-doping, the fibres produced are larger compared to those doped with the individual components. When co-doping with 75 % $AlCl_3$:25 % CoAc and 25 % $AlCl_3$:75 % CoAc, some of the fibres tend to fuse together. However, when doped with 50 % $AlCl_3$:50 % CoAc, almost all the fibres remain separated from one another.

*Energy dispersive X-ray spectroscopy*

An EDX analysis was carried out to determine the elemental composition in ZnAc:$AlCl_3$:PVA and ZnAc:CoAc:PVA, as shown in Figure 5. Based on the analysis results, the element carbon (C) has a higher percentage than other elements, with a value of 52 % (atomic %). The carbon is thought to come from the solvents or the other organic materials used in the synthesis process. The presence of oxygen in the sample indicates the presence of oxide, which is possibly ZnO or Al–O and Co–O based compounds, with a percentage of 25 % (atomic %).

Figure 6 shows the Energy Dispersive X-Ray Spectroscopy (EDX) analysis of ZnAc–$AlCl_3$–CoAc: PVA, including an elemental mapping that illustrates the distribution of elements in $AlCl_3$ and CoAc. The mapping results reveal that the carbon (C) element, shown in red, is present in greater amounts than the oxygen (O) element, which appears in yellowish-green. This suggests that the synthesis process was successful. In contrast, the EDX analysis of the control ZnO shows the following elemental composition: C (52 %), O (25 %), Al (4 %), Si (5 %), Cl (6 %), and Zn (8 %).

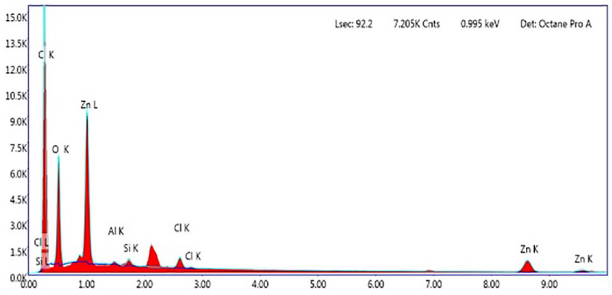


Figure 6. Energy Dispersive X-ray Spectroscopy (EDX) analysis of the ZnAc-$AlCl_3$- CoAc: PVA.

Characterisation – X-ray diffraction (XRD)

The analysis was conducted using a 10 × 10 mm beam and a Cu/Kα X-ray source with a wavelength of $\lambda$ = 1.54060 Å. The equipment operated at 40 kV and 25 mA, with a 2θ angle range of 5° to 90° and increments of 0.02°. During the analysis, the humidity was kept at 53 % and the temperature was maintained at 20.6°C. The X-ray diffraction patterns of ZnO material co-doped with $AlCl_3$ and CoAc are shown in Figure 7. The diffraction patterns obtained are similar, with the highest peaks observed around 2θ = 5.3°, 8.2°–8.4°, 12.1°, 19.4°–19.5°, and 20.0°. These peaks are characteristic of ZnO crystals with a $P6_3mc$ (186) space group structure, according to JCPDS reference No. 36-1451, particularly in the (101) crystal plane. Each sample exhibited a distinct diffraction pattern based on the composition of $AlCl_3$ and CoAc. Samples with a higher CoAc content (0 % $AlCl_3$) showed broader peaks and lower intensity, suggesting a smaller crystallite size or greater amorphous nature.

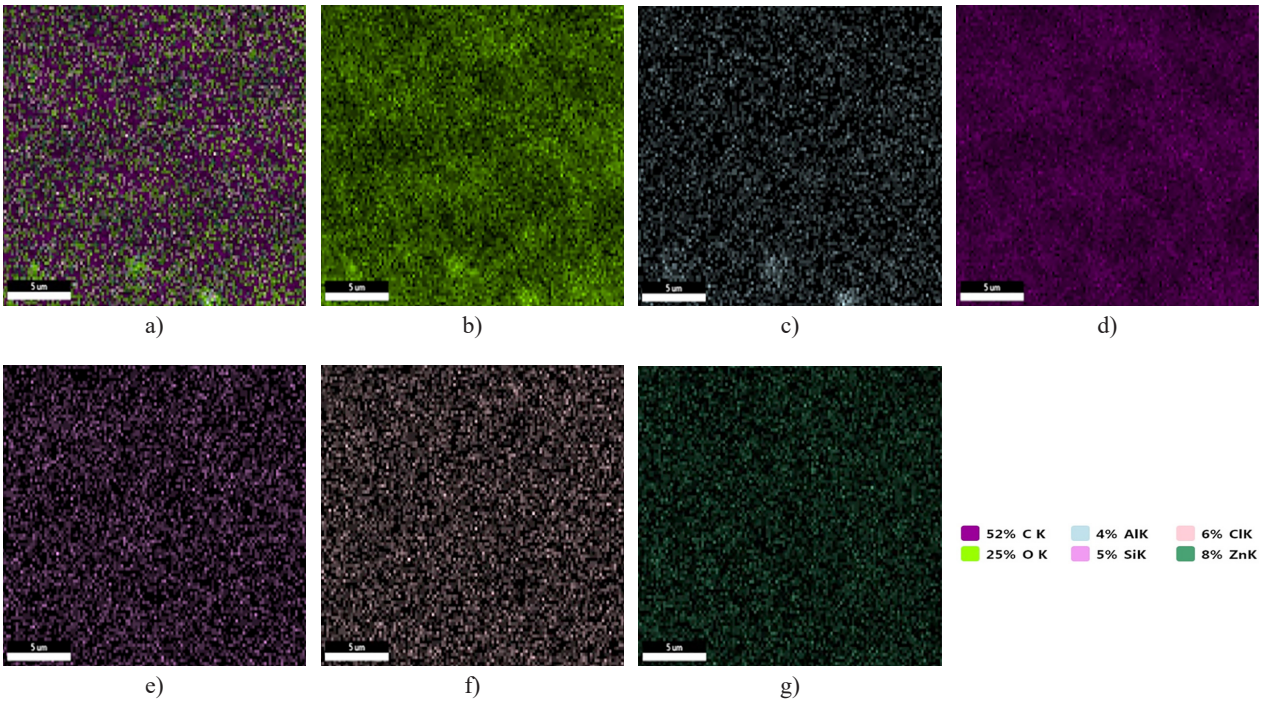


Figure 5. EDX mapping on the nanofibre membranes.

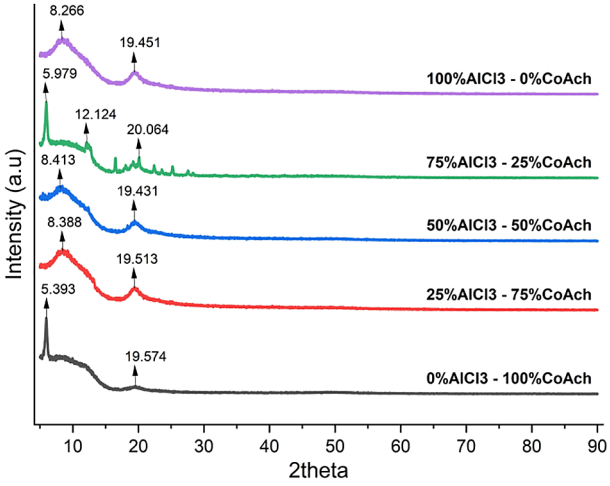


Figure 7. X-ray diffraction patterns of the $AlCl_3$ and CoAc materials.

Conversely, the samples with a higher $AlCl_3$ content (100 % $AlCl_3$) exhibited sharper peaks, indicating increased crystallinity. Diffraction peaks at 2θ = 5.3°, 8.2°––8.4°, and 12.1° may suggest the presence of aluminium or cobalt-based complex compounds, while the main peak at 2θ = 19.4°–19.5° is generally associated with the ZnO structure or other phases resulting from doping.

## Fourier Transform Infrared Spectroscopy (FTIR) characterisation

Figure 8 shows FTIR characterisation of ZnAc: :$AlCl_3$:PVA and ZnAc:CoAc:PVA.

The Fourier Transform Infrared Spectroscopy (FTIR) analysis was performed to identify the functional groups in ZnO doped with $AlCl_3$ and CoAc within the wavenumber range of 500-4000 $cm^{-1}$. The FTIR spectra showed variations in absorption bands based on the dopant composition. The key absorption bands observed include: 2656-2665 $cm^{-1}$ (present in the samples with high CoAc), associated with O–H/C–H vibrations from the residual solvent or precursors; 2160 $cm^{-1}$ (only in the 50 % $AlCl_3$ - 50 % CoAc sample), corresponding to C≡N or C≡C groups in complex compounds; 1765 $cm^{-1}$ (only in the 100 % $AlCl_3$ - 0 % CoAc sample), related to C=O vibrations in the carbonyl group; 667-695 $cm^{-1}$ (found in all the samples), attributed to M–O (Zn–O, Al–O, or Co–O) vibrations; and 430-427 $cm^{-1}$ (appears in 75 % $AlCl_3$ – 25 % CoAc and 50 % $AlCl_3$ – 50 % CoAc), related to the Al-O or Co-O intermetallic interactions. As the CoAc content increases, a new vibration at 2656 $cm^{-1}$ appeared, and the band at 667 $cm^{-1}$ broadens, indicating changes in the crystallinity or molecular interactions. On the other hand, increasing the $AlCl_3$ content results in characteristic vibrations at 1765 $cm^{-1}$, suggesting different phases or bonding types in the material. The 667 $cm^{-1}$ band is a crucial marker for the presence of a metal-oxygen-based phase, which is important for analysing the crystal structure and piezoelectric properties of the material.

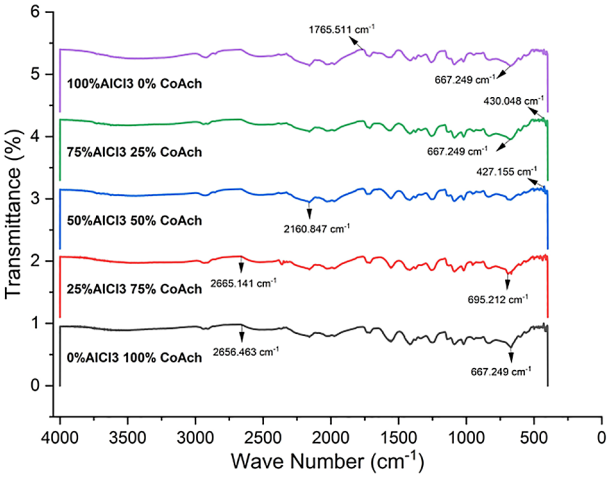


Figure 8. FTIR spectrum for: a) 100 % $AlCl_3$, 0 % CoAc; b) 75 % $AlCl_3$, 25 % CoAc; c) 50 % $AlCl_3$, 50 % CoAc; d) 25 % $AlCl_3$, 75 % CoAc; e) 0 % $AlCl_3$, 100 % CoAc.

## CONCLUSION

ZnO-based electrospun nanofibre membranes doped with $AlCl_3$ and CoAc for piezoelectric nanogenerator applications were successfully fabricated. The PVA precursor solution was prepared by dissolving PVA in distilled water and processed through an electrospinning machine for 10 hours under the following conditions: 13 kV voltage, a 13 cm distance between the drum collector and stainless-steel needle tip, a solution flow rate of 0.5 mL/hour, a collector rotation speed of 125 rpm, and humidity of around 58 %. Nanofibre characterisation using scanning electron microscopy (SEM) showed fibre diameters of 341, 344, 363, 365, and 361 nm. The energy-dispersive X-ray (EDS) analysis confirmed the elemental composition of the membrane: C (52 %), O (25 %), Al (4 %), Si (5 %), Cl (6 %), and Zn (8 %). The X-ray diffraction (XRD) revealed diffraction peaks at approximately 2θ = 5.3°, 8.2°–8.4°, and 12.1°, suggesting the presence of aluminium or cobalt-based complex compounds. The main peak at 2θ = 19.4°–19.5° is associated with the ZnO structure or potential additional phases due to doping. The Fourier Transform Infrared Spectroscopy (FTIR) analysis indicated that increasing the CoAc content resulted in new vibrations at 2656 $cm^{-1}$ and the broadening of the band at 667 $cm^{-1}$, signalling changes in the crystallinity or molecular interactions. On the other hand, increasing the $AlCl_3$ content led to characteristic vibrations at 1765 $cm^{-1}$, suggesting variations in the material's phases or bonding. The presence of a metal-oxygen-based phase plays a crucial role in understanding the crystal structure and piezoelectric properties of the material.

Acknowledgements

*The author would like to express gratitude to all those who contributed to the successful completion of this research. This work was supported by the Directorate of Higher Education in Indonesia through the national competitive research program at Andalas University, which is part of a doctoral dissertation research, under contract number 31/UN16.19/PT.01.03/PDD/2024. The author also extends thanks to the engineering faculty of Universitas Andalas and the National Research and Innovation Agency (BRIN) for providing the necessary equipment for the research characterisation. Additionally, appreciation is given to the Nanoscience and Nanotechnology Research Center of the Bandung Institute of Technology (ITB) and the Manufacturing Engineering Technology Study Program of the Indorama Engineering Polytechnic for their support in the publication of this work.*

## REFERENCES

1. Baek J. H., Park J. Y., Kang J. S., Kim D., Koh S. W., Kang Y. C. (2012): Fabrication and thermal oxidation of ZnO nanofibers prepared via electrospinning technique. *Bulletin of the Korean Chemical Society*, *33*(8), 2694-2698. doi: 10.5012/bkcs.2012.33.8.2694
2. Chang J., Dommer M., Chang C., Lin L. (2012): Piezoelectric nanofibers for energy scavenging applications. *Nano energy*, *1*(3), 356-371. doi: 10.1016/j.nanoen.2012.02.003
3. Chen X., Xu S., Yao N., Shi Y. (2010): 1.6 V nanogenerator for mechanical energy harvesting using PZT nanofibers. *Nano letters*, *10*(6), 2133-2137. doi: 10.1021/nl100812k
4. Chen Y. Q., Zheng X. J., Feng X. (2009): The fabrication of vanadium-doped ZnO piezoelectric nanofiber by electrospinning. *Nanotechnology*, *21*(5), 055708. doi: 10.1088/0957-4484/21/5/055708
5. Choi D., Lee K. Y., Lee K. H., Kim E. S., et al. (2010): Piezoelectric touch-sensitive flexible hybrid energy harvesting nanoarchitectures. *Nanotechnology*, *21*(40), 405503. doi: 10.1088/0957-4484/21/40/405503
6. Chung S. Y., Kim S., Lee J. H., Kim K.,et al. (2012): All-solution-processed flexible thin film piezoelectric nanogenerator. *Advanced Materials (Deerfield Beach, Fla.)*, *24*(45), 6022-6027. doi: 10.1002/adma.201202708
7. Dong Z., Kennedy S. J., Wu Y. (2011): Electrospinning materials for energy-related applications and devices. *Journal of Power Sources*, *196*(11), 4886-4904. doi: 10.1016/j.jpowsour.2011.01.090
8. Fang T. H., Kang S. H. (2010): Physical properties of ZnO: Al nanorods for piezoelectric nanogenerator application. *Current Nanoscience*, *6*(5), 505-511. doi: 10.2174/157341310797574961
9. Haertling G. H. (1999): Ferroelectric ceramics: history and technology. *Journal of the American Ceramic Society*, *82*(4), 797-818. doi: 10.1111/j.1151-2916.1999.tb01840.x
10. Hananto F.S., Santoso D.R., Julius (2011): Application of piezoelectric material film PVDF (polyvinylidene flouride) as liquid viscosity sensor. *Jurnal Neutrino: Jurnal Fisika dan Aplikasinya*. doi: 10.18860/neu.v0i0.1648
11. He J. H., Liu Y., Mo L. F., Wan Y. Q., Xu L. (2008). *Electrospun nanofibres and their applications*. Shawbury, UK: ISmithers.
12. Kanjwal M. A., Sheikh F. A., Barakat,N. A., Li X., Kim H. Y., Chronakis I. S. (2011): $Co_3O_4$, ZnO, $Co_3O_4$–ZnO nanofibers and their properties. *Journal of Nanoengineering and nanomanufacturing*, *1*(2), 196-202.
13. Lee D. Y., Cho J. E., Cho N. I., Lee M. H., Lee S. J., Kim B. Y. (2008): Characterization of electrospun aluminum-doped zinc oxide nanofibers. *Thin Solid Films*, *517*(3), 1262-1267. doi: 10.1016/j.tsf.2008.05.027
14. Pham Q. P., Sharma U., Mikos A. G. (2006): Electrospinning of polymeric nanofibers for tissue engineering applications: a review. *Tissue engineering*, *12*(5), 1197-1211. doi: 10.1089/ten.2006.12.1197
15. Ren H., Ding Y., Jiang Y., Xu F., Long Z., Zhang P. (2009): Synthesis and properties of ZnO nanofibers prepared by electrospinning. *Journal of Sol-Gel Science and Technology*, *52*, 287-290. doi: 10.1007/s10971-009-2030-2
16. Ryan T. P. (2007). *Modern engineering statistics*. John Wiley & Sons.
17. Sangkhaprom N., Supaphol P., Pavarajarn V. (2010): Fibrous zinc oxide prepared by combined electrospinning and solvothermal techniques. *Ceramics International*, *36*(1), 357-363. doi: 10.1016/j.ceramint.2009.09.014
18. Shmueli Y., Shter G. E., Assad O., et al. (2012): Structural and electrical properties of single Ga/ZnO nanofibers synthesized by electrospinning. *Journal of Materials Research*, *27*(13), 1672-1679. doi: 10.1557/jmr.2012.118
19. Sholahuddin I. (2013): Fabrikasi Nanogenerator ZnO Dan AZO Berbasis Serat Nano Dengan Metode Elektrospinning. *Universitas Sebelas Maret*.
20. Sigmund W., Yuh J., Park H., Maneeratana V., et al. (2006): Processing and structure relationships in electrospinning of ceramic fiber systems. *Journal of the American Ceramic Society*, *89*(2), 395-407. doi: 10.1111/j.1551-2916.2005.00807.x
21. Suyitno S., Purwanto A., Lullus Lambang G. Hidayat R., Sholahudin I., Yusuf M., Huda S., Arifin, Z. (2014): Fabrication and characterization of zinc oxide-based electrospun nanofibers for mechanical energy harvesting. *Journal of Nanotechnology in Engineering and Medicine*, *5*(1), 011002. doi: 10.1115/1.4027447
22. Wang Z. L., Wang X., Song J., Liu J., Gao Y. (2008): Piezoelectric nanogenerators for self-powered nanodevices. *IEEE Pervasive Computing*, *7*(1), 49-55. doi: 10.1109/MPRV.2008.14
23. Yang X., Shao C., Guan H., Li X., Gong J. (2004): Preparation and characterization of ZnO nanofibers by using electrospun PVA/zinc acetate composite fiber as precursor. *Inorganic Chemistry Communications*, *7*(2), 176-178. doi: 10.1016/j.inoche.2003.10.035
24. Zhao T., Fu Y., Zhao Y., Xing L., Xue X. (2015): Ga-doped ZnO nanowire nanogenerator as self-powered/active humidity sensor with high sensitivity and fast response. *Journal of Alloys and Compounds*, *648*, 571-576. doi: 10.1016/j.jallcom.2015.07.035
25. Burmawi, et al. (2020): Material density of composite hydroxyapatite bovine bone-borosilicate formed by compaction and sintering techniques. In *IOP Conference Series: Materials Science and Engineering* (Vol. 990, No. 1, p. 012024): doi: 10.1088/1757-899X/990/1/012024

26. Gunawarman, et al. (2019): Synthesis and characterization of calcium precursor for hydroxyapatite synthesis from blood clam shell (Anadara antiquata) using planetary ball mill process. In *IOP Conference Series: Materials Science and Engineering* (Vol. 602, No. 1, p. 012072). IOP Publishing. doi: 10.1088/1757-899X/602/1/012072
27. Ihamdi, et al. (2023): Effect of bilayer nano-micro hydroxyapatite on the surface characteristics of implanted Ti–6Al–4V ELI. *International Journal of Automotive and Mechanical Engineering*, *20*(3), 10777-10785. doi: 10. 15282/ijame.20.3.2023.19.0833
28. Burmawi et al. (2020): Material density of composite hydroxyapatite bovine bone-borosilicate formed by compaction and sintering techniques. In *IOP Conference Series: Materials Science and Engineering* (Vol. 990, No. 1, p. 012024). IOP Publishing. doi: 10.1088/1757-899X/990/1/012024
29. Indra A., Gunawarman, Affi J., Mulyadi I.H., Wiyanto Y. (2021): Physical and mechanical properties of hydroxyapatite ceramics with a mixture of micron and nano-sized powders: Optimising the sintering temperatures. *Ceram-Silikaty*, *65*(3), 224-234. doi: 10.13168/cs.2021.0022
30. Saravanakumar B., Mohan R., Thiyagarajan K., Kim S. J. (2013): Fabrication of a ZnO nanogenerator for eco-friendly biomechanical energy harvesting. *RSC advances*, *3*(37), 16646-16656. doi: 10.1039/C3RA40447A
31. Mukhadis A., Suhartadi S., Sutadji E., Puspitasari P. (2017): Effectiveness of professional practice work with discovery learning methods in engineering program D IV automotive safety. *Advanced Science Letters*, *23*(2), 1154-1157. doi: 10.1166/asl.2017.7524
32. Suyitno S., Purwanto A., Lullus Lambang G. Hidayat R., Sholahudin I., Yusuf M., Huda S., Arifin Z. (2014): Fabrication and characterization of zinc oxide-based electrospun nanofibers for mechanical energy harvesting. *Journal of Nanotechnology in Engineering and Medicine*, *5*(1), 011002. doi: 10.1115/1.4027447
33. Yetri Y., Gunawarman G., Rakiman R., Rivai A. Y., Nur I. (2024): Investigation of the Adsorption Characteristics of Theobroma cacao Peels Biomass Inhibitors on Mild Steel Surfaces by EIS, SEM-EDX, XPS, and Chemical Studies in Acidic Media. *Solid State Phenomena*, *357*, 69-82. doi: 10.4028/p-qz0pLd